AGE-RELATED CHANGES IN THE EFFECTIVE STIFFNESS OF THE HUMAN THORAX USING FOUR LOADING CONDITIONS

Richard Kent, Chris Sherwood, David Lessley, Brian Overby
University of Virginia

Fumio Matsuoka
Toyota Motor Corporation

ABSTRACT

This paper presents a series of tests utilizing ten post-mortem human surrogates (PMHS) to study the effective stiffness (k_{eff}) of the thorax at realistic restraint loading rates (~1 m/s) under four loading conditions (distributed load, diagonal belt, 4-point belt, and hub). Subjects were grouped into four subgroups: younger males (n = 2, age $\leq$ 54 years), younger females (n = 2, age $\leq$ 58 years), older males (n = 3, age $\geq$ 75), and older females (n = 3, age $\geq$ 79). It is shown that k_{eff} is strongly dependent on the loading condition, with the lowest k_{eff} corresponding to the hub loading condition (k_{eff} = 4,750 N/ 100% deflection). The highest k_{eff} was measured with the distributed loading condition (3.1 times hub k_{eff}), followed by the 4-point belt (3.0), and the diagonal belt (2.1). The effect of age was small compared to the influence of size, but the older subjects exhibited slightly higher k_{eff} than the younger subjects of similar size, indicating a slight trend toward increasing k_{eff} as a person ages.

Key Words: Aging, thorax, rib fractures, restraint systems, stiffness

LIFE EXPECTANCY IN THE U.S. HAS DOUBLED since the beginning of the 20th century (Oskvig 1999) and by 2030, 25% of the population will be age 65 or older (OECD 2001). People are driving later in life and a vehicle has become an important source of independence and mobility. In fact, nearly one-fifth of new car buyers in the U.S. are over 60 years of age (Alonso-Zaldivar 2000), and this proportion is increasing.

Protecting an older occupant in a collision presents a unique set of challenges. It is well documented that, in general, older people are more susceptible to injury than younger, and that the morbidity, mortality, and treatment costs for a given injury are typically higher for older people than for younger (see, for example, Martinez et al. 1994, Miltner and Salwender 1995, Peek-Asa et al. 1998, Miller et al. 1998, Bulger et al. 2000). Another characteristic that distinguishes the older U.S. population is its propensity to wear seat belts (Figure 1). While this behavior certainly provides an overall benefit, an aging person can become increasingly susceptible to thoracic injury, primarily rib fractures, from seat belt loading in a crash (Evans 1989, Zhou et al. 1998).

The ease with which ribs fracture and the ability to recover from rib fractures both change substantially as a person ages. In the young, the material and geometric characteristics of the ribs result in a structure that is relatively difficult to damage. Likewise, the young have efficient blood-oxygen exchange and higher pain tolerance, which increase their ability to tolerate rib fractures and damage to the underlying lung parenchyma. Aging, on the other hand, is associated with an increase in the pressure required for a given amount of pulmonary respiratory volume and a decrease in thoracic muscle mass, which lead to decreased effective cough and an inability to clear secretions. Furthermore, as a person ages, cardiac output decreases and the alveoli coalesce, resulting in a reduction of small airways in the bronchial tree. Finally, aging is associated with atrophy of the epithelium lining the bronchi, which predisposes an older person to chronic colonization of the upper airway with bacteria. All of these factors facilitate the development of pneumonia and other sequelae following rib fractures.

As a first step toward developing the specific biomechanical knowledge required to optimize restraints and to minimize rib fracture risk for older people, Kent et al. (2003) found that the chest deflection threshold for rib fractures is strongly dependent on age, but insensitive to the load distribution on the chest. They quantified this age dependence for both the onset of rib fractures and for more than six fractures (Figure 2). The question that follows from this finding is whether there is also an age-related change in the effective thoracic stiffness. The force required to generate an

injurious level of chest deformation is often assumed to change with age and load distribution, but these changes have not been quantified in detail. Bone material properties, pulmonary compliance, thoracic geometry, organ material properties, and cartilage ossification all change with age, but it is not known how these factors combine to change the global force-deformation characteristics of the thorax. The purpose of the current study is to address this issue by quantifying the effective thoracic stiffness (k_{eff}) for post-mortem human surrogates (PMHS) over an age range and for different loading conditions on the chest.

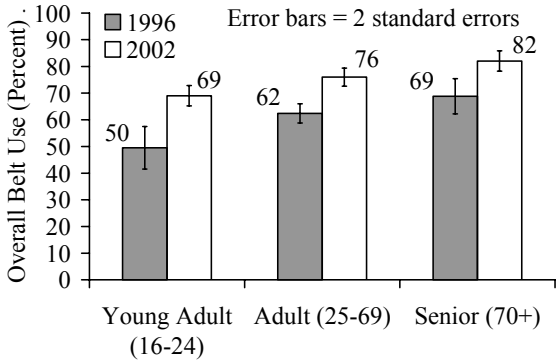

Figure 1. Belt use rate in 1996 and in 2002 for three age groups in the U.S. Data from Glassbrenner (2003) and NHTSA (1997).

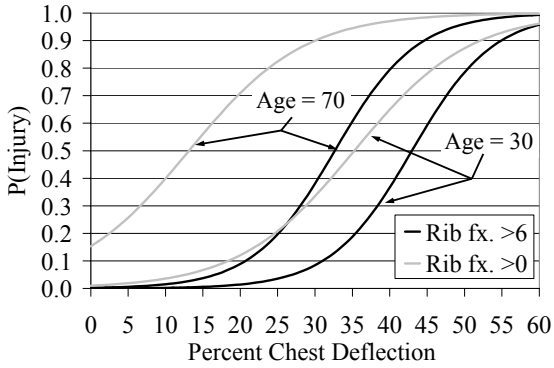

Figure 2. Injury threshold sensitivity to age (from Kent et al. 2003). Two ages (30 and 70) and two levels of injury (any rib fracture, more than six rib fractures) are shown.

METHODS

TEST APPARATUS AND LOADING CONDITIONS: Ten PMHS (Table 1) were subjected to each of four loading conditions on the anterior thorax (Figure 3): diagonal belt loading, distributed loading, 4-point belt loading, and hub loading (note: one of the subjects was not loaded with the 4-point belt). A hydraulic master-slave cylinder arrangement with a high-speed material testing machine (Instron model 8874, Canton, Massachusetts) was used to generate chest deflection at a rate similar to that experienced by restrained PMHS in 48 km/h frontal sled tests (Figure 4).

Diagonal belt, 4-point belt, and distributed loading were performed via cable-belt systems. All belts were constructed of spectra fiber-reinforced sail cloth, which did not strain during loading. The 5-cm-wide diagonal belt passed over the left shoulder and crossed the anterior thorax approximately 45° from the sagittal plane. The belt engaged the clavicle at approximately the proximal third, crossed the midline approximately mid-sternally, and exited the body laterally at approximately the superior-inferior location of the 9th rib. The 4-point belt condition involved a second diagonal belt oriented symmetrically to the diagonal belt described above. For distributed loading, a 20.3-cm-wide lateral belt loaded the area approximately between the second and seventh ribs. The hub load was applied with a 15.2-cm diameter steel circular plate intended to mimic the loading surface described by Kroell et al. (1974). The center of the hub was located at the intersection of the mid-sagittal plane and approximately the 4th interstitial space. The hub edges were beveled to reduce edge stresses. A frame with a bearing track was used with the hub condition to ensure anterior-posterior loading and to prevent the hub from rotating during loading.

Chest deflection was measured anteriorly via string potentiometers attached to the loading belts or to the hub. For the hub loading condition, deflection was measured at a single point. For all other loading conditions, deflection was measured at three points (upper left, middle, lower right). In this paper, the mid-sternal chest deflection is used to calculate the effective stiffness. The location of the mid-sternal chest deflection measurement is given by Y_{notch}, defined as the distance from the sternal notch inferiorly along the mid-sternum. This distance was constant for all loading conditions on each subject. The mid-sternal deflection matches the middle string attachment site for the diagonal belt and 4-point belt conditions, while it was obtained via interpolation between the upper and middle potentiometers for the distributed loading condition.

Table 1. Description of PMHS Subjects

	Younger Males		Younger Females		Older Males			Older Females		
PMHS ID	145	187	157	186	170	189	190	176	177	182
Age at Death/Gender	54/M	54/M	55/F	58/F	75/M	79/M	79/M	85/F	79/F	80/F
Mean ± 1 S.D.	54.0 ± 0.0		56.5 ± 2.1		77.7 ± 2.3			81.3 ± 3.2		
Mass (kg)	87.7	112.7	74.4	61.2	65.3	56.7	73.5	58.2	47.6	65.3
Mean ± 1 S.D.	100.2 ± 17.7		67.8 ± 9.3		65.2 ± 8.4			57.0 ± 8.9		
Stature (cm)	192	178	168	178	178	159	173	157	161	157
Mean ± 1 S.D.	185.0 ± 9.4		172.7 ± 7.2		169.8 ± 9.8			157.8 ± 2.3		
BMI	23.9	35.4	26.5	19.4	20.6	22.4	24.7	23.8	18.5	26.7
Mean ± 1 S.D.	29.7 ± 8.2		22.9 ± 5.0		22.6 ± 2.0			23.0 ± 4.1		
Chest Depth (mm) (4^{th} rib/8^{th} rib)	210/ 235	220/ 252	228/ 240	161/ 161	195/ 220	198/ 208	225/ 230	195/ 205	150/ 180	200/ 210
Chest Depth (mm) (5^{th} rib, inflated)*	244	251	235	186	243	254	245	211	180	220
Mean ± 1 S.D.	247.5 ± 4.9		210.5 ± 34.6		247.3 ± 5.9			203.7 ± 21.0		
Chest Breadth (mm) (4^{th} rib/8^{th} rib)	392/ 340	349/ 368	321/ 299	260/ 275	305/ 330	313/ 304	326/ 332	320/ 345	330/ 310	320/ 340
Cause of Death†	Glio-blastoma Multi-forme	Cardio-respira-tory Arrest	Emphy-sema	Organ Failure (NFS)	MI	Septi-cemia	MI	COPD	Lung Can-cer	Cong. Heart Fail.
Bone Density §	NA	359.5	NA	233.5	212.1	263.9	316.6	NA	94.0	127.5

* The chest depth at the 4^{th} and 8^{th} ribs was measured without pulmonary pressurization. The chest depth at the 5^{th} rib, with the inflated lungs, is defined as c_{init} and used as the chest depth for normalizing chest deflection as a percentage of chest depth (see Equation 2).

† MI – Myocardial infarction, COPD – Chronic obstructive pulmonary disease

§Houndsfield units from calibrated CT scan of lumbar vertebra (NA – Not Available)

TEST SUBJECTS AND TEST STRATEGY: Age, size, gender, and cause-of-death criteria were used to select the subjects for testing. The causes of death for all subjects are unlikely to have degraded tissue properties significantly pre-mortem. The unembalmed subjects were preserved either by freezing or by refrigeration prior to testing. To model the *in vivo* condition as much as practicable, the subjects' pulmonary systems were pressurized to typical mean inspiration pressure (10 kPa) immediately prior to testing. Pressurization was accomplished via a tracheostomy and the airway remained occluded throughout loading. To facilitate handling, the subjects' lower extremities were amputated at the femur mid-shaft. All PMHS testing and handling procedures were approved by the University of Virginia (UVA) institutional review board.

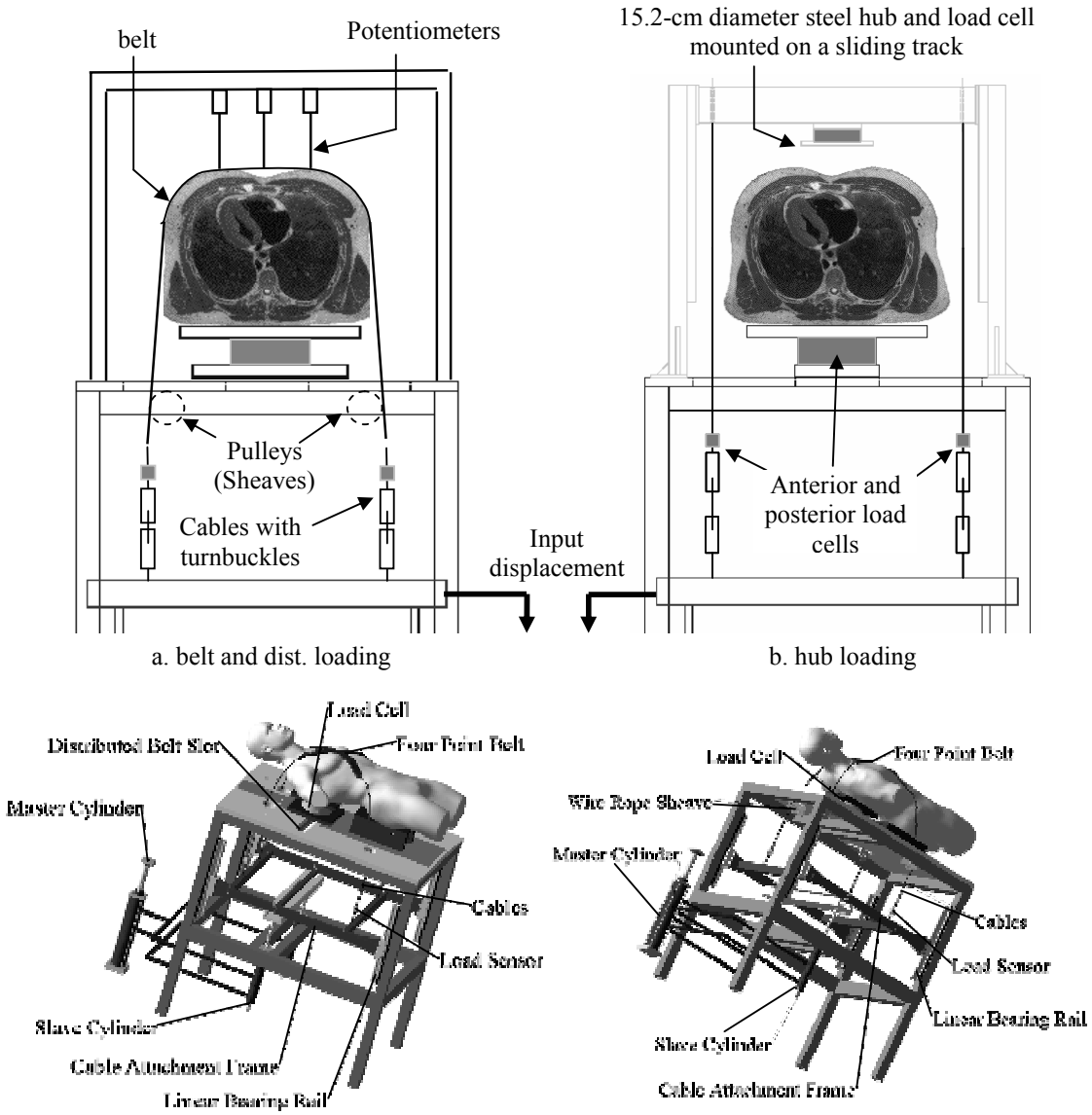

Figure 3.Schematic depictions of test fixture and loading conditions (small triangles represent string potentiometer attachment sites).

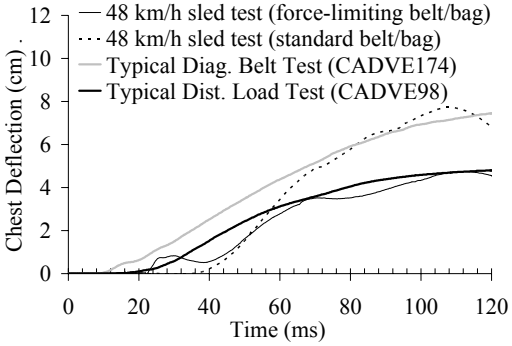

Figure 4. Comparison of deflection-time histories from two PMHS sled tests (see Kent et al. 2001) and typical tests performed using the apparatus shown in Figure 3.

Table 2 – Location of Mid-Sternal Deflection Measurement Used in k_{eff} Calculations

Subject	145	187	157	186	170	189	190	176	177	182
Y_{notch} (cm)*	9.5	7.8	6.0	5.0	5.8	9.8	9.0	5.6	7.1	6.5

*Y_{notch} is the inferior distance from the sternal notch to point at which the mid-sternal chest deflection used in all effective stiffness calculations is measured (see Figure 3). It is constant for all loading conditions. This point corresponds to the attachment site of the string potentiometer for the diagonal belt and 4-point belt loading conditions. For the distributed loading condition, the deflection at this point is determined by interpolating between the upper left and mid-sternal deflection measurements.

To maximize the applicability of the structural models (i.e., to approach injury levels), but minimize thoracic response changes due to tissue damage, tests were designed to approach, but not exceed, rib fracture threshold for all tests except a final, injurious test on each PMHS (Table 3). Since the rib fracture threshold varies widely depending on the subject's age, gender, size, bone condition, and the presence of superficial soft tissues, the applied displacement varied among subjects. The lack of rib fractures was verified using an acoustic sensor and palpation after each loading cycle. The order in which the various loading conditions were tested was randomized to minimize the effect of test order and timing. Furthermore, prior to each test, a 10-cycle, 1-Hz sinusoid having the same magnitude deflection was used to precondition the thorax and further minimize the importance of test order. The final, injurious test performed on each subject involved a repeat of one of the loading conditions tested earlier.

In addition to the string potentiometers described above, thoracic instrumentation included load cells measuring the cable tension and hub forces as well as load cells mounted posteriorly to measure the force generated by the deforming thorax. Data were sampled at 5 kHz.

In this paper, the instantaneous effective stiffness, k_{inst}, is defined as the time-varying ratio:

$$k_{inst}(t) = \frac{F_{post}(t)}{D_{norm}(t)} \qquad [1]$$

where

$F_{post}(t)$ is the reaction force measured posteriorly (see Figure 3) and $D_{norm}(t)$ is the ratio of the mid-sternal chest deflection, c_{mid}, (measured at a distance Y_{notch} inferior of the sternal notch) to the initial chest depth, c_{init}, where c_{init} was measured at the nominal location of the fifth rib with the lungs inflated to 10 kPa, c_{init}:

Table 3 – Test Matrix†

Test	Subject	Loading Condition	Test	Subject	Loading Condition
CADVE54	145	diagonal belt	CADVE163	182	diagonal belt
CADVE57	145	Distributed	CADVE165	182	4-pt belt
CADVE62	145	Hub	CADVE167	182	distributed
CADVE64	145	hub*	CADVE171	182	hub
CADVE176	157	Distributed	CADVE174	182	diagonal belt*
CADVE179	157	Hub	CADVE190	186	4-pt belt
CADVE182	157	diagonal belt	CADVE192	186	diagonal belt
CADVE184	157	4-pt belt	CADVE195	186	distributed
CADVE188	157	4-pt belt *	CADVE197	186	hub
CADVE87	170	Hub	CADVE201	186	hub*
CADVE90	170	4-pt belt	CADVE217	187	hub
CADVE93	170	diagonal belt	CADVE221	187	distributed
CADVE96	170	Distributed	CADVE223	187	4-pt belt
CADVE98	170	distributed*	CADVE225	187	diagonal belt
CADVE152	176	Hub	CADVE228	187	diagonal belt*
CADVE155	176	Distributed	CADVE242	189	4-pt belt
CADVE157	176	4-pt belt	CADVE246	189	diagonal belt
CADVE159	176	diagonal belt	CADVE248	189	hub
CADVE161	176	diagonal belt*	CADVE250	189	distributed
CADVE139	177	diagonal belt	CADVE252	189	distributed*
CADVE141	177	4-pt belt	CADVE230	190	hub
CADVE143	177	Distributed	CADVE232	190	distributed
CADVE146	177	Hub	CADVE234	190	diagonal belt
CADVE149	177	hub*	CADVE236	190	4-pt belt
			CADVE240	190	4-pt belt *

†Thorax was preconditioned prior to each test. *Last test on all subjects was a test to injury.

$$D_{norm}(t) = \frac{c_{mid}(t)}{c_{init}} \quad [2].$$

For the purposes of comparing loading conditions and test subjects, the constant effective stiffness, k_{eff}, is defined as the slope of a linear regression to the F_{post}-D_{norm} cross plot. In reality the slope of this line is not constant, but over the deflection range considered here the assumption of linearity is adequate to illustrate trends. The linearity assumption is not appropriate, however, for the final, injurious test performed on each subject. As a result, these tests are not considered in the relative comparison of k_{eff} for the different loading conditions. They are, however, presented in Appendix A to illustrate the repeatability of the test setup and to quantify the force-deflection response at injurious levels, albeit for a single loading condition per subject.

RESULTS

In all tests, the target deflection levels were obtained and reasonable reaction forces were measured (Appendix A). The maximum input deflection, D_{norm}, ranged from 7.8% to 44.8%. The posterior reaction force, F_{post}, ranged from 489 N (hub, subject 186, 58F, 61.2 kg) to 3832 N (distributed, subject 170, 75M, 65.3 kg). The effective stiffness ranged from 2873 N/100% (hub, subject 189, 79M, 56.7 kg) to 20988 N/100% (4-point belt, subject 187, 54M, 112.7 kg) (Table 4).

Table 4 – Peak values and k_{eff}

Test	Maximum c_{mid}, mm and (D_{norm}, %)	Maximum Force, N	k_{eff}, N†	Test	Maximum c_{mid}, mm and (D_{norm}, %)	Maximum Force, N	k_{eff}, N†
CADVE54	38.9 (15.9)	2413	14252	CADVE163	27.3 (12.4)	1321	9919
CADVE57	37.9 (15.5)	3364	19763	CADVE165	29.2 (13.3)	1989	13359
CADVE62	48.5 (19.9)	1379	5644	CADVE167	23.1 (10.5)	1772	16611
CADVE64	86.9 (35.6)	3319	*	CADVE171	35.7 (16.2)	905	4352
CADVE176	44.9 (19.1)	1633	7385	CADVE174	90.0 (40.9)	2871	*
CADVE179	51.0 (21.7)	1431	5424	CADVE190	21.4 (11.5)	1348	11482
CADVE182	44.8 (19.1)	1431	6459	CADVE192	18.6 (10.0)	738	7125
CADVE184	47.5 (20.2)	2279	9367	CADVE195	14.6 (7.8)	1247	15098
CADVE188	62.7 (26.6)	3271	*	CADVE197	21.5 (11.6)	489	3020
CADVE87	48.9 (20.1)	1042	4106	CADVE201	62.6 (33.7)	3806	*
CADVE90	47.1 (19.4)	3033	14208	CADVE217	41.3 (16.5)	1081	5029
CADVE93	48.9 (20.0)	2107	9327	CADVE221	34.5 (13.8)	3028	20453
CADVE96	32.8 (13.5)	2320	16631	CADVE223	37.0 (14.7)	3257	20988
CADVE98	60.4 (24.8)	3832	*	CADVE225	36.8 (14.7)	2433	15420
CADVE152	34.3 (16.3)	1532	8259	CADVE228	51.3 (20.5)	3813	*
CADVE155	30.7 (14.6)	2344	15713	CADVE242	36.8 (14.5)	1759	11374
CADVE157	36.1 (17.1)	2407	13850	CADVE246	37.1 (14.6)	1243	7102
CADVE159	31.0 (14.7)	1081	6496	CADVE248	37.1 (14.6)	579	2873
CADVE161	89.4 (42.4)	3298	*	CADVE250	25.4 (10.0)	1352	13708
CADVE139	33.3 (18.5)	1665	8788	CADVE252	75.3 (29.6)	3590	*
CADVE141	24.7 (13.7)	1708	10884	CADVE230	28.9 (11.8)	779	5108
CADVE143	19.6 (10.9)	1348	12502	CADVE232	25.3 (10.3)	1741	16110
CADVE146	31.2 (17.3)	846	3687	CADVE234	31.3 (12.8)	1894	13728
CADVE149	80.5 (44.8)	3327	*	CADVE236	35.9 (14.6)	2935	17840
				CADVE240	53.6 (21.8)	3585	*

†Determined from regression as described in text. k_{eff} is not a ratio of the maximum deflection and force listed here. The units of k_{eff} are Newtons per deflection per initial chest depth (or N/100% deflection). For example, the force at 20% deflection would be k_{eff}*0.2.

*Linear stiffness not appropriate for injury tests due to non-linearity at higher deflection levels.

EFFECT OF LOADING CONDITION: The effective stiffness was found to be strongly dependent on the loading condition, with consistent trends observed for all subjects. The distributed and 4-point belt conditions, which were not significantly different from each other, resulted in significantly higher k_{eff} than either the diagonal belt or the hub (Table 5). The hub resulted in significantly lower k_{eff} than the diagonal belt (Figure 5).

EFFECT OF PMHS CHARACTERISTICS: When all loading conditions were grouped, the younger male group had the greatest mean k_{eff}, followed by the older males and then the older females (Figure 5). Interestingly, the younger females had a lower k_{eff} than the two older groups, though this trend was not significant (Table 5). The younger female group did attain significance compared to the younger male group, however, with a p value of 0.049 indicating a significantly lower k_{eff}.

COMBINED EFFECTS: In an attempt to assess the combined effects of PMHS characteristics and loading condition, the four age and gender groups were evaluated separately for all loading conditions. Again, consistent trends among loading conditions were observed, with the distributed and 4-point belt conditions resulting in higher forces for a given level of chest deflection (Figure 6).

Table 5 – p Values for Single-tailed Heteroscedastic t-tests of Difference Between Groups* (**bold** = $p < 0.05$)

All Loading Conditions Grouped

	YF	OF	OM
YM	**0.049**	0.128	0.151
OF	0.120	NA	0.372
OM	0.087	0.372	NA

All Subjects Grouped

	Hub	Diag. Belt	4-Pt Belt
Distributed	**<0.001**	**0.001**	0.166
Diag. Belt	**<0.001**	NA	**0.016**
4-pt Belt	**<0.001**	**0.016**	NA

Loading Condition and Sex/Age Group

	YF	OF	OM
	Distributed		
YM	0.131	**0.029**	**0.009**
OF	0.264	NA	0.371
OM	0.239	0.371	NA
	Diagonal Belt		
YM	**0.003**	**0.006**	0.071
OF	0.134		0.253
OM	0.120	0.253	
	4-pt Belt		
YM	NA	NA	NA
OF	0.123	NA	0.228
OM	0.078	0.228	NA
	Hub		
YM	0.267	0.477	0.083
OF	0.281	NA	0.218
OM	0.450	0.218	NA

*YF = Younger females, OF = Older females, OM = Older males, YM = Younger males

Variability among subjects was observed, however, within the four age/gender groups. In particular, the younger female group exhibited a wide range, while the other groups were more repeatable across subjects (Figure 7). The mean effective stiffness exhibited some significant differences among groups. The younger male group was significantly stiffer than either of the older groups with the distributed load and was significantly stiffer than either of the female groups with the diagonal belt loading. No significant trends were observed with the 4-point or hub loading conditions, though some p values below 0.1 (indicating marginal significance) were found, as shown in Table 5.

DISCUSSION

The structural characteristics of the thorax have been studied since the 1960s but, due to low rates of seatbelt use, early studies focused on loading experienced by unbelted subjects (e.g., Kroell et al. 1974). As seatbelt use increased, researchers recognized the need to evaluate thoracic response under belt loading and at lower loading rates. The primary source of response data for diagonal belt loading is the test series presented by L'Abbe et al. (1982) and Cesari and Bouquet (1990, 1994), which involved a series of PMHS positioned supine on a table and subjected to seatbelt-like loading via a pendulum and cable system. For the purposes of dummy and computer model validation, however, both the Kroell tests and the Cesari and Bouquet tests have limitations, some of which the present study has attempted to address. First, tests of multiple loading conditions on the same subject were not performed in either of those earlier test series. A second limitation of the available blunt hub data is that they consist largely of impact tests in which only the anterior force was measured. When the thorax is subjected to an impact and the force is measured at the impacting surface, large inertial forces are measured prior to significant deformation of the thorax. As a result, the characteristic thoracic force-deflection corridor is dominated by the inertial response early in the corridor and it is difficult to isolate the effective thoracic stiffness. This characteristic of the data limits its usefulness in many contemporary applications. In the case of seatbelt loading, for example, there is never an impact between the belt and the thorax and the thoracic response has a smaller inertial component.

LOADING CONDITION-SPECIFIC EFFECTIVE STIFFNESS: The data presented here define the effective stiffness (albeit at a single loading rate) for multiple loading conditions on a single subject and therefore provide important information for assessing the biofidelity of physical and computation thoracic models. The use of the posterior reaction force rather than the anteriorly applied force minimizes the inertial contribution to the response. There is an inertial effect in these tests, however, as evidenced by the oscillations that can be seen in the early portion of the force-deflection cross-plots. This effect is small, however, and the effective stiffness can be quantified by fitting a line through the inertial oscillations. The data presented here are not, however, sufficient to separate the elastic and viscous characteristics of the thorax since the measured effective stiffness is due to a combination of these characteristics. Research aimed at isolating the elastic and viscous characteristics is currently ongoing at the University of Virginia and will be presented in a future paper.

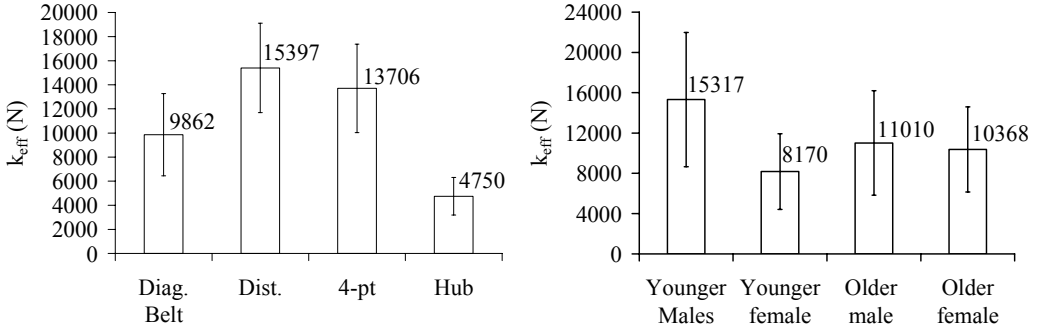

Figure 5. Mean effective stiffness (all subjects) ± one standard deviation.

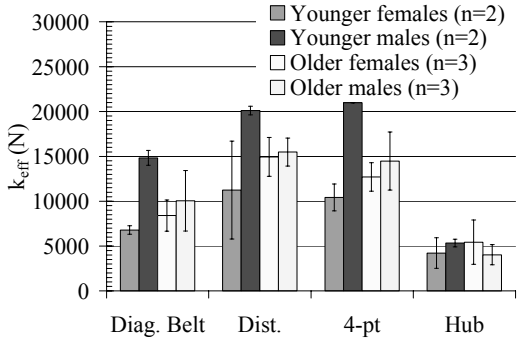

Figure 6. Effective stiffness (mean ± one st .dev.) for all loading conditions and age/gender groups.

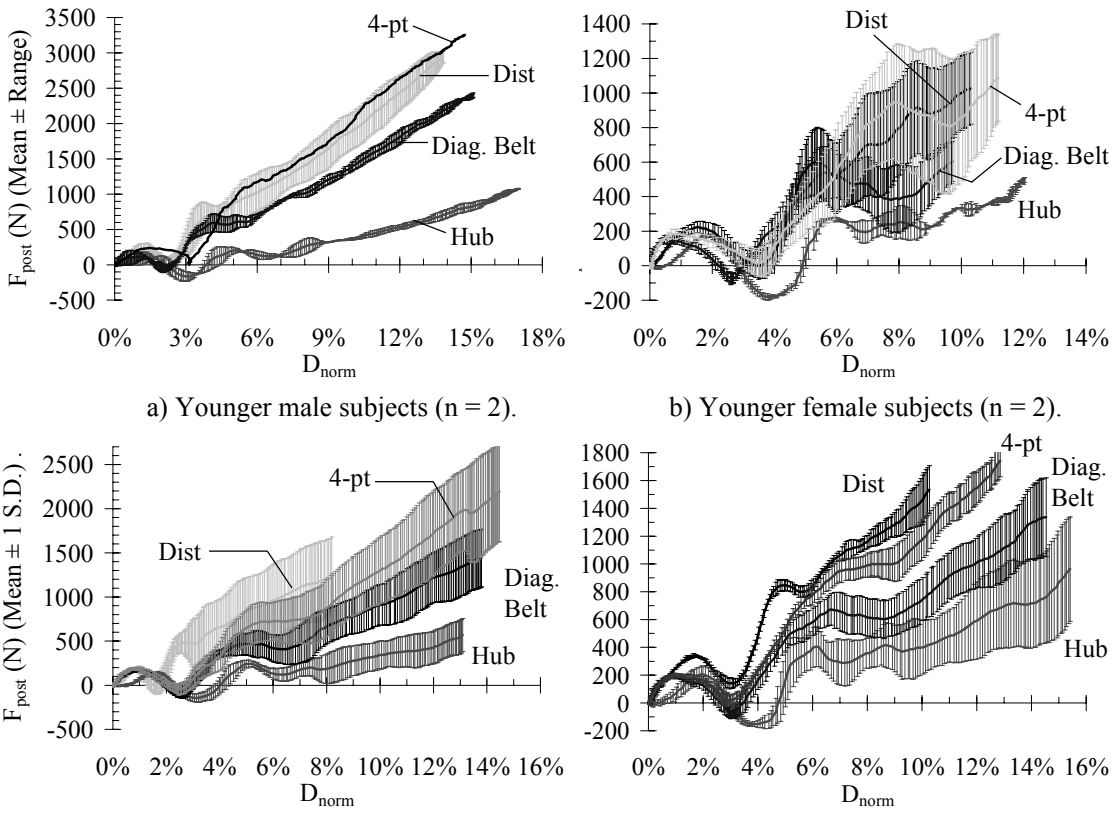

a) Younger male subjects (n = 2).

b) Younger female subjects (n = 2).

c) Older male subjects (n = 3).

d) Older female subjects (n = 3).

Figure 7. Force-deflection cross-plots of all non-injury tests.

The finding that the loading condition strongly influences the thoracic response is supported by numerous studies (e.g., Patrick et al. 1965, Bierman et al. 1946, Fayon et al. 1975) and is intuitively correct. We believe this is the first study, however, to quantify the change in response for the same subject loaded by different conditions to levels approaching rib fracture threshold. Our finding that the hub load generates a lower effective stiffness than the other conditions was expected due to the difference in the loaded area. The hub engages only approximately 180 cm^2, while the diagonal belt engages 250 cm^2, the 4-point configuration engages 460 cm^2, and the distributed load engages 730 cm^2. The area of load application does not completely explain the observed differences in effective stiffness, however. For both subjects, the 4-point belt and distributed conditions generated similar effective stiffness despite a large difference in loaded area. It is apparent that the specific anatomical structures that are engaged play at least as large a role as the loaded area. The 4-point belt engages the short and thick upper ribs as well as the clavicles. These stiff structures were not engaged by either the hub or the distributed load.

EFFECT OF AGE, GENDER, AND SIZE: The number of tests presented here is insufficient to completely define the changes in thoracic stiffness that may occur as a person ages. In fact, this study has shown that variations in individual thoracic stiffness are due to many factors in addition to age. For example, the younger males in this study were approximately 30 kg heavier on average than the subjects in the other groups. This large size differential is arguably the dominant factor contributing to the significantly stiffer response measured for these subjects. A marginally significant ($p = 0.086$) age influence can still be seen, however, if only the other three groups (younger females, older males, older females), which are all similar in size, are considered (Table 6).

Table 6. Multivariate Linear Regression Results

Sample	Outcome	Predictors	Coefficient	p
All subjects except the younger males	keff	Intercept	-8513	0.428
		Age (years)	147.73	0.086
		Mass (kg)	122.3	0.244

Interestingly, the trend is toward a stiffer response for the older subjects once the larger, younger males are removed (increase in k_{eff} of approximately 100 N/year) (Table 6 and Figure 5, right chart). While the number of subjects is too few to state definitively what effect aging has on thoracic stiffness, it can be stated that this study provides no evidence that thoracic stiffness should be assumed to decrease with age. As mentioned in the introduction, there are many factors that contribute to the global thoracic response of the thorax. Some of these factors (e.g., decreasing elastic modulus of bone) would tend to decrease the global thoracic stiffness while others (e.g., calcification of the costal cartilage) may tend to increase it. The fairly recent availability of computed tomography (CT) scans and three-dimensional reconstructions of thoracic cage geometry for large numbers of subjects has identified another potentially important factor. Currently unpublished research at the University of Michigan has identified an anecdotal trend of changing rib slope as a function of age (Wang 2003). Younger subjects tend to exhibit pronounced posterior-to-anterior rib slope in a lateral CT reconstruction, while older subjects tend to exhibit less slope (i.e., the ribs are closer to perpendicular to the spine) (Figure 8). The mechanisms of this change are not currently understood, but a dramatic geometric change would be expected to have a large effect on the global effective thoracic stiffness under anterior loading. In fact, a pronounced geometric change like that illustrated in Figure 8 would likely dominate changes in material properties, in addition to dramatically influencing rib fracture mechanisms and chest deflection tolerance levels. In other words, both thoracic stiffness and chest deflection injury tolerance level may be strongly dependent on factors other than the well documented age-related changes in bone modulus and failure properties. Additional work is needed in order to understand how the relative contributions of geometry and material properties dictate the global effective thoracic stiffness values measured in this study. To this end, CT reconstructions of the 10 test subjects presented here are currently being analyzed and material characterization tests of isolated rib segments are planned.

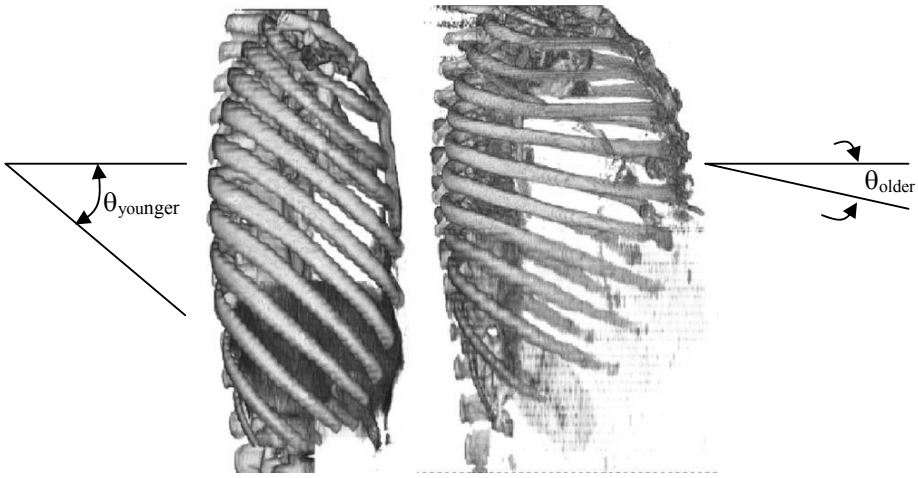

Figure 8. CT reconstructed lateral views of thoracic cage of a 17 year-old female (left) and a 64 year-old male (right) illustrating age-related change in rib slope (images courtesy of Dr. Stewart Wang, University of Michigan).

TEST METHODOLOGY AND LIMITATIONS: Despite attempts to avoid injury prior to the final test, there were cases of acoustic emissions consistent with isolated rib fractures prior to the final test. This was of concern since the rib cage loses stability as ribs progressively fracture and the restraint-specific thoracic stiffness values could potentially by skewed by test order. The issue of response changes due to repeated tests was addressed in three ways in this study. First, the order in which the various conditions were tested was varied among subjects so that the effect of test order could be separated from the effect of load distribution. Second, the thorax was pre-conditioned prior to each test. Finally, a single loading condition was repeated for each subject. The effectiveness of this strategy is supported by the fact that test order is not a significant predictor of trends in k_{eff} ($p = 0.437$). Furthermore, while fractures did occur during some of the "non-injury" tests, the effect of these fractures is negligible. The relative ranking of loading conditions is reasonably consistent among subjects regardless of the order in which the conditions were tested and the final injurious test was consistent with the force-deflection response measured in the earlier, non-injury test. The repeated test methodology used here therefore appears to be valid for modeling thoracic stiffness up to chest deflection levels approaching (and even exceeding slightly) the rib fracture threshold.

The use of non-injury tests to define the relative stiffness is a necessary limitation of repeated testing. As the injury tests clearly show, a linear extrapolation of the non-injury data does not satisfactorily predict the response at substantially larger levels of chest deflection (see Appendix A). For the purpose of modeling or predicting the onset of rib fractures, however, these non-injury tests are considered to be adequate.

Limitations of the PMHS tests presented here include the use of a constrained back condition, which may result in different response than a thorax loaded only by its inertia, as it is in most frontal car crashes. One possible effect of the posterior boundary is an increase in stiffness due to constraint of the costovertebral articulations, though to our knowledge this increase has never been shown and is likely small compared to inter-specimen variability and inter-test variability. It is also unlikely that this increase in stiffness, if present, would differ among the loading conditions evaluated here and therefore skew the assessment of relative stiffness.

CONCLUSIONS

This study resulted in two findings of primary importance. First, the effective stiffness of the thorax is strongly dependent on the load distribution. This dependence is due primarily to the particular anatomical structures that bear the load and secondarily to the area of load application. Loading conditions that involve the upper ribs and shoulders generate effectively stiffer response than

loading conditions that do not. Four loading conditions were evaluated here. Their ranking from stiffest to least stiff is

1. distributed load (15,397 N/100% deflection),
2. 4-point belt load (13,706 N/100% deflection),
3. diagonal belt load (9,862 N/100% deflection), and
4. hub load (4,750 N/100% deflection).

The other primary finding of this study is that the effective thoracic stiffness is not strongly dependent on age, though a marginally significant trend of increasing stiffness with increasing age was observed. The size of the subject was found to be a much more important factor, with larger subjects exhibiting stiffer response. This finding is not universal, however, since factors such as rib cage geometry and superficial soft tissue depth also play a role. Future research in this area should include consideration of how age-related geometric and bone material property changes influence global thoracic response.

REFERENCES

Alonso-Zalvidar, Ricardo. (2000) Auto Makers Retool to Fit an Aging U.S. Los Angeles Times, July 31.

Bierman, H.R., Wilder, R.M., Hellems, H.K. (1946) The physiological effects of compressive forces on the torso. Report #8, Naval Medical Research Institute Project X-630, Bethesda, MD.

Bulger, E., Arneson, M., Mock, C., Jurkovich, G. (2000) Rib fractures in the elderly. The Journal of Trauma 48:1040-1047.

Cesari, D. and Bouquet, R. (1990) Behavior of human surrogates under belt loading. Proc. 34th Stapp Car Crash Conference, pp. 73-82, Society of Automotive Engineers, Warrendale, PA.

Cesari, D. and Bouquet, R., (1994) Comparison of Hybrid III and human cadaver thoracic deformations." Proceedings of the 38th Stapp Car Crash Conference, Paper 942209, Society of Automotive Engineers, Warrendale, PA.

Evans, L. (1989) Airbag effectiveness in preventing fatalities predicted according to type of crash, driver age, and blood alcohol concentration. 33rd Annual Proceedings of the Association for the Advancement of Automotive Medicine, AAAM, Des Plaines, IL.

Fayon, A., Tarriere, C., Walfisch, G., Got, C., Patel, A. (1975) Thorax of 3-point belt wearers during a crash (experiments with cadavers). Paper 751148, Society of Automotive Engineers, Warrendale, PA.

Glassbrenner, D. (2003) Safety belt use in 2002 – demographic characteristics. NHTSA Research Note, DOT HS 809 557, Washington, DC.

Kent, R., Crandall, J., Bolton, J., Prasad, P., Nusholtz, G., Mertz, H. (2001) The influence of superficial soft tissues and restraint condition on thoracic skeletal injury prediction. Stapp Car Crash Journal 45:183-203.

Kent, R., Patrie, J., Poteau, F., Matsuoka, F., Mullen, C. (2003) Development of an age-dependent thoracic injury criterion for frontal impact restraint loading. Paper 72, 18th Technical Conference on the Enhanced Safety of Vehicles, Nagoya, Japan.

Kroell, C., Schneider, D., Nahum, A. (1974) Impact tolerance and response of the human thorax II. Paper number 741187, Society of Automotive Engineers, Warrendale, Pennsylvania.

L'Abbe, R., Dainty, D., Newman, J., (1982) An experimental analysis of thoracic deflection response to belt loading." Proceedings of the 7th International Research Council on the Biomechanics of Impact Conference, Bron, France, pp. 184-194.

Martinez, R., Sharieff, G., Hooper, J. (1994) Three-point restraints as a risk factor for chest injury in the elderly. Journal of Trauma – Injury, Infection, and Critical Care 37:980-984.

Miller, T., Lestina, D., Spicer, R. (1998) Highway crash costs in the United States by driver age, blood alcohol level, victim age, and restraint use. Accident Analysis and Prevention 30:137-150.

Miltner, E., and Salwender, H.-J. (1995) Influencing factors on the injury severity of restrained front seat occupants in car-to-car head-on collisions. Accident Analysis and Prevention 27:143-150.

NHTSA (1997) National occupant protection use survey – 1996 controlled intersection study. NHTSA Research Note, Washington DC.

OECD (2001) Ageing and Transport – Mobility Needs and Safety Issues. Organization for Economic Co-operation and Development. Paris, France.

Oskvig, R. (1999) Special problems in the elderly. Chest 115:158S-164S.

Patrick, L.M., Kroell, C.K., Mertz, H.J. (1965) Forces on the human body in simulated crashes. Proc. 9th Stapp Car Crash Conference, pp. 237-260.

Peek-Asa, C., Dean, B., Halbert, R. (1994) Traffic-related injury hospitalizations among California elderly, 1994. Accident Analysis and Prevention 30:389-395.

Wang, S. (2003). Personal Communication.

Zhou, Q., Rouhana, S., Melvin, J. (1996) Age effects on thoracic injury tolerance. Paper 962421, Society of Automotive Engineers, Warrendale, PA.

APPENDIX A – TIME HISTORIES OF FORCE AND DEFLECTION DATA

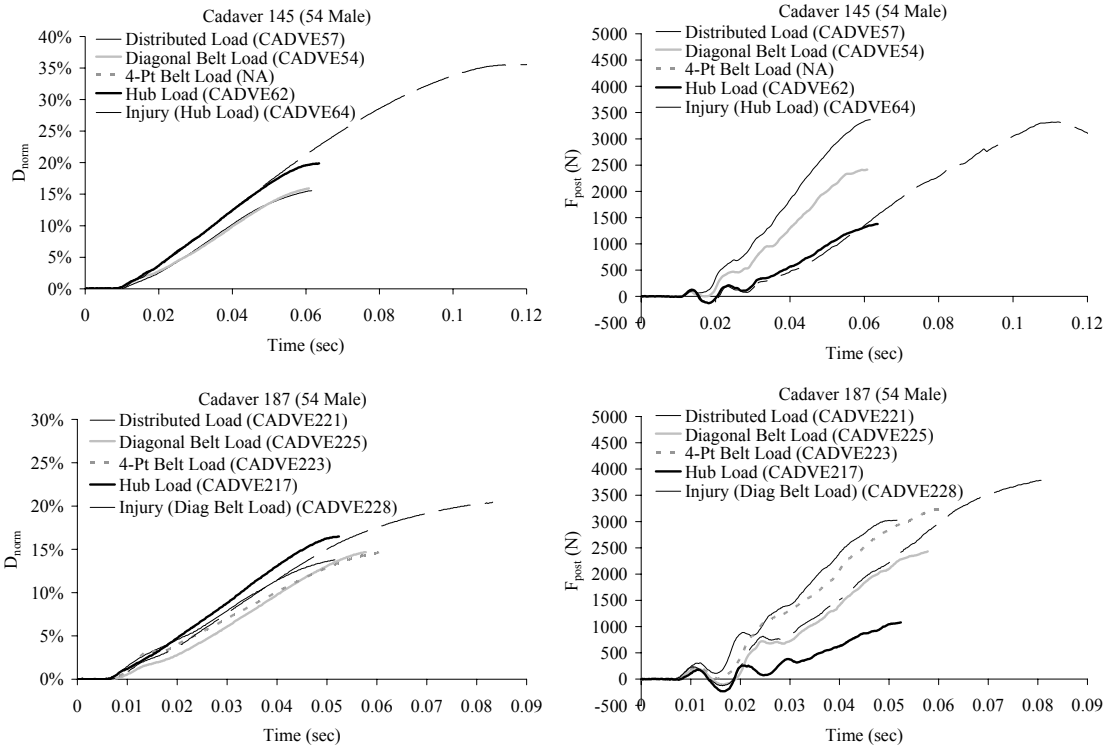

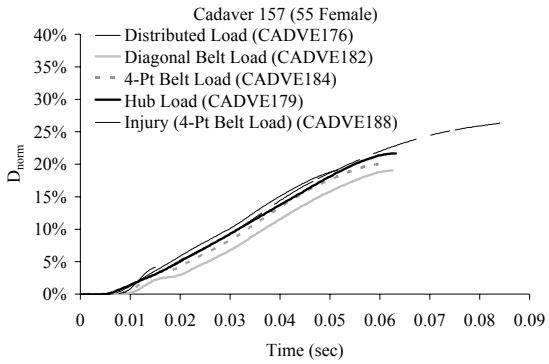
Cadaver 157 (55 Female)
Distributed Load (CADVE176)
Diagonal Belt Load (CADVE182)
4-Pt Belt Load (CADVE184)
Hub Load (CADVE179)
Injury (4-Pt Belt Load) (CADVE188)
D_norm
Time (sec)

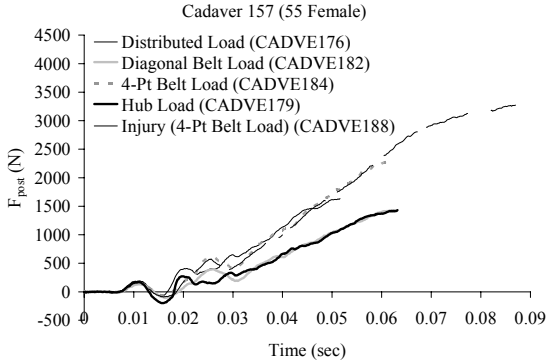
Cadaver 157 (55 Female)
Distributed Load (CADVE176)
Diagonal Belt Load (CADVE182)
4-Pt Belt Load (CADVE184)
Hub Load (CADVE179)
Injury (4-Pt Belt Load) (CADVE188)
F_post (N)
Time (sec)

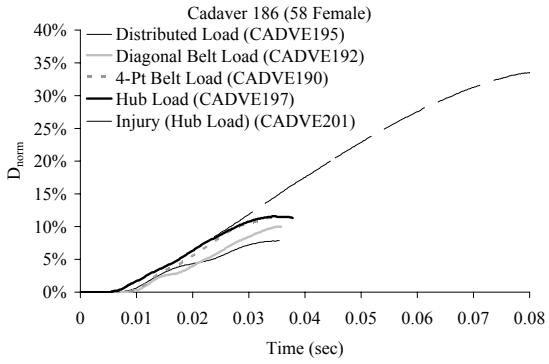
Cadaver 186 (58 Female)
Distributed Load (CADVE195)
Diagonal Belt Load (CADVE192)
4-Pt Belt Load (CADVE190)
Hub Load (CADVE197)
Injury (Hub Load) (CADVE201)
D_norm
Time (sec)

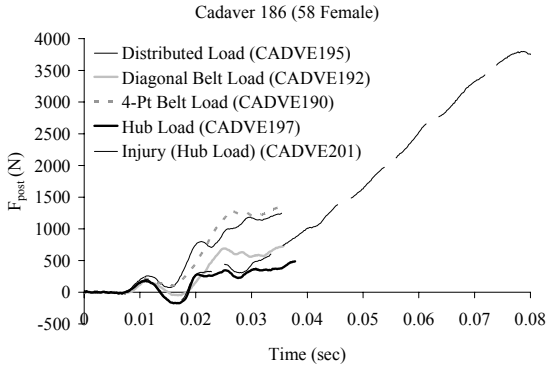
Cadaver 186 (58 Female)
Distributed Load (CADVE195)
Diagonal Belt Load (CADVE192)
4-Pt Belt Load (CADVE190)
Hub Load (CADVE197)
Injury (Hub Load) (CADVE201)
F_post (N)
Time (sec)

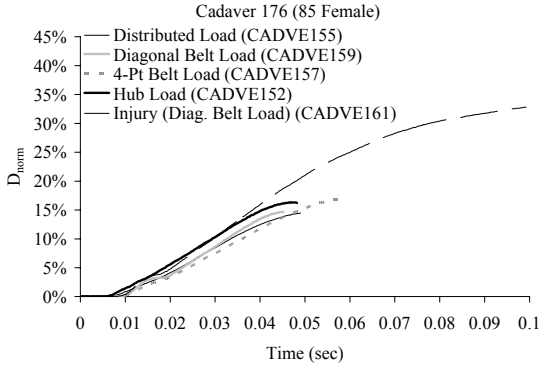
Cadaver 176 (85 Female)
Distributed Load (CADVE155)
Diagonal Belt Load (CADVE159)
4-Pt Belt Load (CADVE157)
Hub Load (CADVE152)
Injury (Diag. Belt Load) (CADVE161)
D_norm
Time (sec)

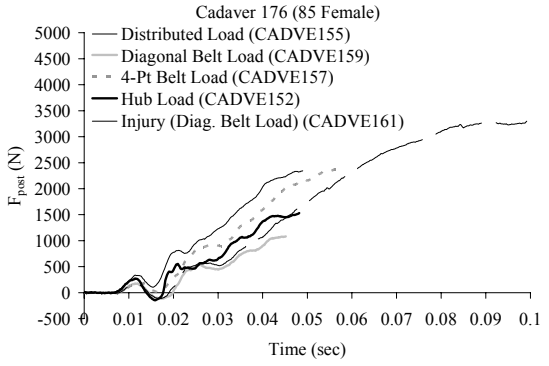
Cadaver 176 (85 Female)
Distributed Load (CADVE155)
Diagonal Belt Load (CADVE159)
4-Pt Belt Load (CADVE157)
Hub Load (CADVE152)
Injury (Diag. Belt Load) (CADVE161)
F_post (N)
Time (sec)

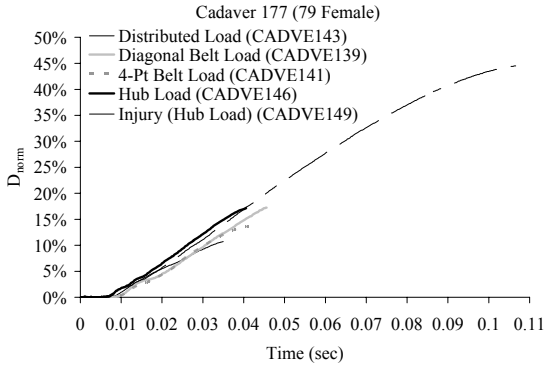
Cadaver 177 (79 Female)
Distributed Load (CADVE143)
Diagonal Belt Load (CADVE139)
4-Pt Belt Load (CADVE141)
Hub Load (CADVE146)
Injury (Hub Load) (CADVE149)
D_norm
Time (sec)

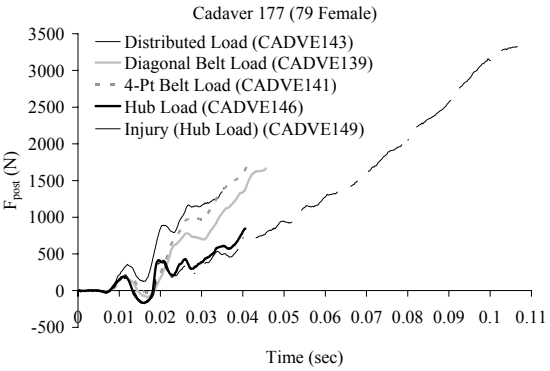
Cadaver 177 (79 Female)
Distributed Load (CADVE143)
Diagonal Belt Load (CADVE139)
4-Pt Belt Load (CADVE141)
Hub Load (CADVE146)
Injury (Hub Load) (CADVE149)
F_post (N)
Time (sec)

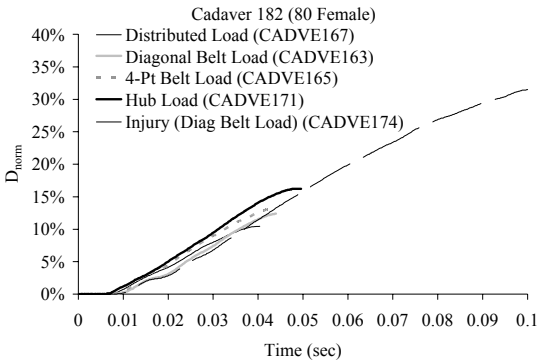
Cadaver 182 (80 Female)
Distributed Load (CADVE167)
Diagonal Belt Load (CADVE163)
4-Pt Belt Load (CADVE165)
Hub Load (CADVE171)
Injury (Diag Belt Load) (CADVE174)
D_norm
Time (sec)

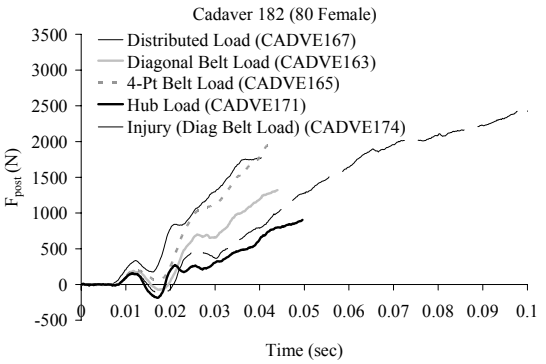
Cadaver 182 (80 Female)
Distributed Load (CADVE167)
Diagonal Belt Load (CADVE163)
4-Pt Belt Load (CADVE165)
Hub Load (CADVE171)
Injury (Diag Belt Load) (CADVE174)
F_post (N)
Time (sec)

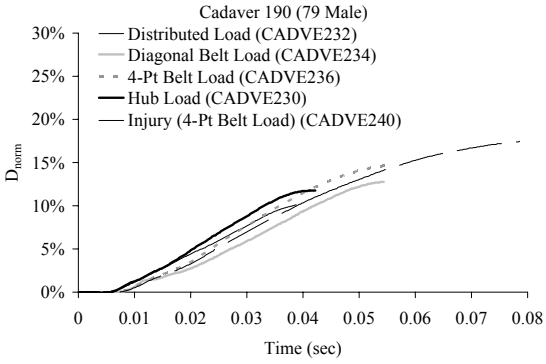
Cadaver 190 (79 Male)
Distributed Load (CADVE232)
Diagonal Belt Load (CADVE234)
4-Pt Belt Load (CADVE236)
Hub Load (CADVE230)
Injury (4-Pt Belt Load) (CADVE240)
D_norm
Time (sec)

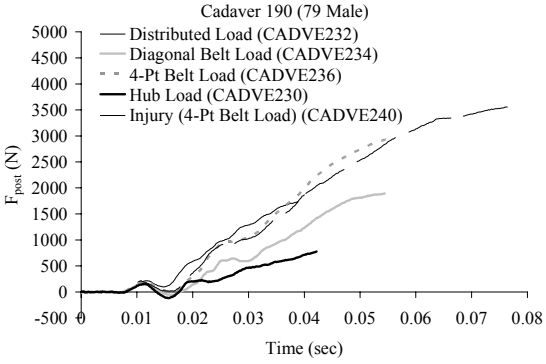
Cadaver 190 (79 Male)
Distributed Load (CADVE232)
Diagonal Belt Load (CADVE234)
4-Pt Belt Load (CADVE236)
Hub Load (CADVE230)
Injury (4-Pt Belt Load) (CADVE240)
F_post (N)
Time (sec)

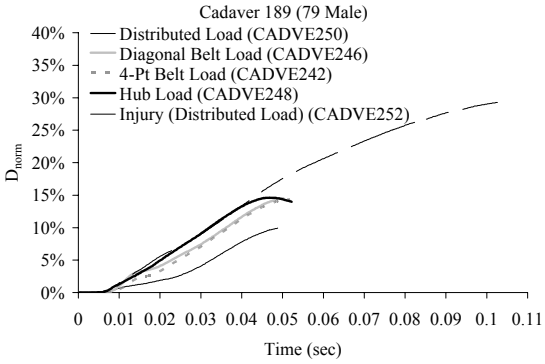
Cadaver 189 (79 Male)
Distributed Load (CADVE250)
Diagonal Belt Load (CADVE246)
4-Pt Belt Load (CADVE242)
Hub Load (CADVE248)
Injury (Distributed Load) (CADVE252)
D_norm
Time (sec)

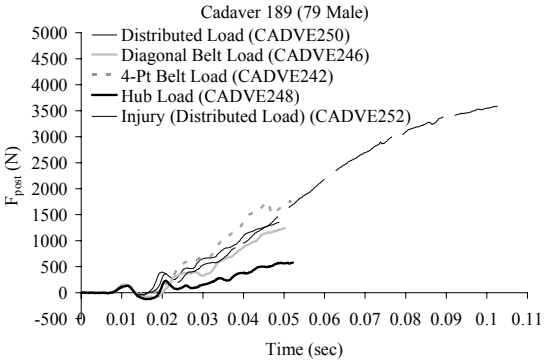
Cadaver 189 (79 Male)
Distributed Load (CADVE250)
Diagonal Belt Load (CADVE246)
4-Pt Belt Load (CADVE242)
Hub Load (CADVE248)
Injury (Distributed Load) (CADVE252)
F_post (N)
Time (sec)

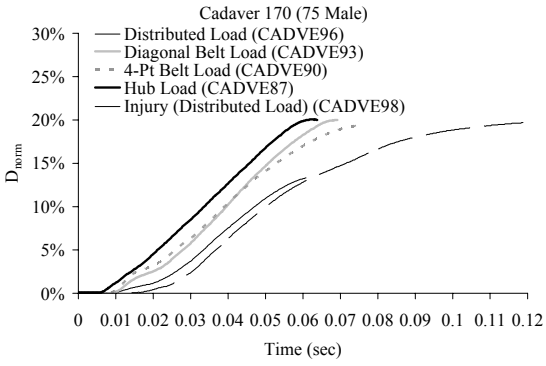
Cadaver 170 (75 Male)
Distributed Load (CADVE96)
Diagonal Belt Load (CADVE93)
4-Pt Belt Load (CADVE90)
Hub Load (CADVE87)
Injury (Distributed Load) (CADVE98)
D_norm
Time (sec)

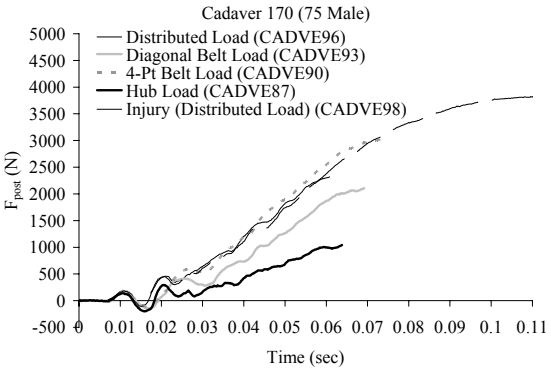
Cadaver 170 (75 Male)
Distributed Load (CADVE96)
Diagonal Belt Load (CADVE93)
4-Pt Belt Load (CADVE90)
Hub Load (CADVE87)
Injury (Distributed Load) (CADVE98)
F_post (N)
Time (sec)